EARTH SURFACE PROCESSES AND LANDFORMS
Earth Surf. Process. Landforms **37**, 169–179 (2012)

Published online 27 September 2011 in Wiley Online Library
(wileyonlinelibrary.com) DOI: 10.1002/esp.2229

A new approach for linking event-based upland sediment sources to downstream suspended sediment transport

Peng Gao* and James Puckett
Department of Geography, Syracuse University, Syracuse, NY, USA

Received 30 November 2010; Revised 9 August 2011; Accepted 31 August 2011

*Correspondence to: Peng Gao, Department of Geography, Syracuse University, Syracuse, NY 13244, USA. E-mail: pegao@maxwell.syr.edu

ESPL
Earth Surface Processes and Landforms

ABSTRACT: In this study, we proposed a new approach for linking event sediment sources to downstream sediment transport in a watershed in central New York. This approach is based on a new concept of spatial scale, sub-watershed area (SWA), defined as a sub-watershed within which all eroded soils are transported out without deposition during a hydrological event. Using (rainfall) event data collected between July and November, 2007 from several SWAs of the studied watershed, we developed an empirical equation that has one independent variable, mean SWA slope. This equation was then used to determine event-averaged unit soil erosion rate, $Q_{S/A}$, (in kg/km^2/hr) for all SWAs in the studied watershed and calculate event-averaged gross erosion E_{ea} (in kg/hr). The event gross erosion E_t (in kilograms) was subsequently computed as the product of E_{ea} and the mean event duration, T (in hours) determined using event hydrographs at the outlet of the studied watershed. Next, we developed two linear sediment rating curves (SRCs) for small and big events based on the event data obtained at the watershed outlet. These SRCs, together with T, allowed us to determine event sediment yield SY_e (in kilograms) for all events during the study period. By comparing E_t with SY_e, developing empirical equations (i) between E_t and SY_e and (ii) for event sediment delivery ratio, respectively, we revealed the event dynamic processes connecting sediment sources and downstream sediment transport. During small events, sediment transport in streams was at capacity and dominated by the deposition process, whereas during big events, it was below capacity and controlled by the erosion process. The key of applying this approach to other watersheds is establishing their empirical equations for $Q_{S/A}$ and appropriately determining their numbers of SWAs. Copyright © 2011 John Wiley & Sons, Ltd.

KEYWORDS: suspended sediment load; sediment rating curve; sediment connectivity; sub-watershed area; event sediment yield; event gross erosion

Introduction

Soil erosion and associated sediment transport have increased worldwide primarily due to land use change (Ramankutty and Foley, 1999; Owens *et al*., 2005). Generally, eroded soils are transported from source areas into stream channels, some deposit and are resuspended later, while others travel through the stream network of a watershed. In-stream sediment inversely affects stream biotic communities and water quality (Russell *et al*., 2001; Bilotta and Brazier, 2008), contaminates drinking water (Gauthiera *et al*., 1999), and impedes river navigation (Wren *et al*., 2007). However, much of in-stream sediment is from upland point sources such as mass movement (de Vente *et al*., 2006) and non-point sources such as agricultural fields, mining sites, and urban regions (Quilbe *et al*., 2008) from which soil erosion and sediment transport are spatially and temporally variable (Van Dijk and Bruijnzeel, 2005; Wilkinson *et al*., 2009; Moreno-de las Heras *et al*., 2010). Thus, understanding the dynamic links between these sources and downstream transport is critical for a variety of watershed management practices such as soil and water conservation, reservoir sedimentation, river restoration, and land-use planning (Pimentel *et al*., 1995; Fryire *et al*., 2007; Jain and Tandon, 2010; Medeiros *et al*., 2010).

A common approach for linking sediment sources to downstream sediment loads is incorporating hysteresis analysis with the development of sediment rating curves (Langlois *et al*., 2005; Lecce *et al*., 2006; Lefran *et al*., 2007; Sadeghi *et al*., 2008; Smith and Dragovich, 2009; Oeurng *et al*., 2010). The former refers to temporal patterns of watershed discharge, Q, and sediment concentration, C, during hydrological events (Williams, 1989), while the latter is the statistical relationship between Q and C (Gao, 2008). Although this approach is capable of exposing the cause–effect relationship between sediment sources and downstream sediment loads, it requires detailed information about hydrological events, Q and C (Salant *et al*., 2008), which is not applicable to watersheds that have not been intensively monitored. An alternative approach relies on the sediment fingerprinting technique to identify quantitatively the relative contribution of different sediment sources to the downstream sediment transport (Walling, 1999; Collins and Walling, 2004). This technique assumes that sediment sources can be discriminated in terms of their geochemical properties or fingerprints and their relative importance may be determined by comparing the fingerprints in the samples from downstream sediment with those from the sources (Collins and Walling, 2004). The technique has been successfully used to construct sediment budget (Rustomji, 2006), identify time-integrated (Salant *et al.*, 2007; Mizugaki *et al.*, 2008; Wilson *et al.*, 2008) and event-based sediment sources (Russell *et al.*, 2001; Martinez-Carreras *et al.*, 2010). However, the good composite mixing models established using this technique for identifying sediment sources generally require substantial data analysis and intricate statistical methods, and hence are mainly appropriate for extensively studied watersheds.

Identification of sediment sources and characterization of transport processes have also been studied using processed-based watershed models (Singh, 1995; Merritt *et al.*, 2003; Aksoy and Kavvas, 2005; Keesstra *et al.*, 2009), which may be divided into lumped and distributed models based on the spatial arrangement (Gao, 2008). Distributed models have received much more attention due to their capacity of accurately describing various physical processes with mathematical equations. However, some theoretical problems and practical limitations emerge subsequently. One fundamental flaw is that physically based laws (usually displayed as governing equations in these watershed models) for hydrological and sediment transport processes are only valid in a very small scale (control volume), which is even smaller than the finest cell size used in distributed models. Therefore, the scale of theories always mismatches that of the observable variables (Beven, 2002). The other ties to the fact that model input parameters are not always known – that is, models represent open systems that have multiple outcomes and hence are impossible to be verified (Oreskes *et al.*, 1994). Consequently, since most process-based models only predict and validate sediment loads at the outlet of a watershed this often leads to the problem of predicting the correct results for the wrong reasons (Bloschl, 2001; Jetten *et al.*, 2003). Thus, developing new watershed models with more accurate description of each transport process may not necessarily result in more accurate prediction of suspended sediment loads (De Roo, 1998; Jetten *et al.*, 2003; Carpenter and Georgakakos, 2006).

In many watersheds lacking of hydrological and sediment monitoring due to financial constraint and limited labor, sediment-related watershed management can only rely on limited data. Relatively simple approaches that can reasonably characterize the dynamic processes of sediment transport within a watershed are thus valuable. In this study, we developed one such approach to reveal the event-based dynamic links between sediment source areas and the downstream sediment transport in a watershed located in central New York, USA.

This approach is based on a new concept, sub-watershed area (SWA). SWA is a spatial scale in which all eroded soils due to various hillslope and in-channel processes are transported out of it without deposition during a single hydrological event. SWA is different from the traditional spatial scale, representative elementary area (REA) that stands for the area in the order of 1 km^2 in which spatial heterogeneity is statistically insignificant (Wood *et al.*, 1988; Bloschl *et al.*, 1995; Woods and Sivapalan, 1995; Merz and Plate, 1997). It can be less or greater than 1 km^2. SWA is also distinct from the fashionable spatial scale, hydrological response unit (HRU) (Dooge, 1968; Flugel, 1995; Bongartz, 2003), which represents an area in which the change of hydrological dynamics is small with respect to its surrounding areas and hence can be regarded as homogeneous. It is much greater than an HRU. A fundamental distinction between SWA and the other two is that the former retains the geomorphological unit, watershed, which facilitates the separation of hillslope processes from in-channel ones.

Based on this concept, we first developed an empirical equation to estimate event sediment loads from all SWAs of the studied watershed and used this equation to determine event gross erosion. Then, we established sediment rating curves (SRCs) for estimating event sediment yield of the watershed. By comparing both among rainfall events, we identified various event-based processes linking hillslope sediment sources to the downstream sediment transport.

Study Area

Oneida Creek watershed is one of seven sub-watersheds comprising Oneida Lake watershed in central New York. It is located in the southwest of the Oneida Lake watershed and has an area of 387 km^2 (Figure 1a). With an elongated geometry, the Oneida Creek watershed extends upstream to the southwest and joins at the outlet to the Oneida Lake. Watershed elevations range from 123 to 574 m, with much higher topographic variations in the upstream region and relatively gentle slope in the downstream area. The watershed has a typical dendric stream network with a drainage density of 1·3 and its main stream, Oneida Creek, is joined by the major branch, Sconondoa Creek (Figure 1b). The mean annual precipitation is more than 1270 mm and annual peak discharges are dominated by rainfall in summer and fall and snowmelt events in spring. After more than 50 years of development, the land use in the Oneida Creek watershed has changed significantly towards agricultural and urban uses, which currently occupy about 55% of the total area. Consequently, sediment load in the Oneida Creek is greater than is usually associated with natural landscapes typical of central New York (Makarewicz and Lewis, 2003). Although the Oneida Creek only contributes 7% of the total water inflow to the Oneida Lake, it supplies about 22·3% of the total sediment load (about 215 tons of soil per storm day) to the lake (Makarewicz and Lewis, 2003). Both the Oneida and Sconondoa Creeks have been listed as prior water bodies for treatment (CNYRPDB, 2004). The needs for effectively controlling sediment load necessitate better understanding of sediment transport processes and source distribution.

In this study, we selected the middle and upper portion of the Oneida Creek watershed, which has an area of about 311 km^2, as the studied watershed (Figure 1b) for two reasons. First, the US Geological Survey (USGS) gauging station available near (upstream of) the outlet facilitates data collection. Second, this portion has diverse land use and significantly variable physiographic conditions, which warranty the spatial diversity of suspended sediment loads required for developing an empirical equation.

Methods

Data collection and preparation

Sampling and geomorphologic survey

We collected event-based water discharge and suspended sediment data at two spatial scales: the outlet of the studied watershed and a group of headwater sub-watersheds that mainly contain order-one or -two streams [the stream order was assigned based on the Strahler's method (Strahler, 1952)]. To ensure the selected sub-watersheds have diverse physiographic conditions available in the studied watershed, we created a preliminary geographic information system (GIS) index map for all sub-watersheds in which the index is a linear combination of topological wetness index (TWI) (Beven and Kirkby, 1979; Beven, 1997) and soil conservation service curve number (CN) (USDA-SCS, 1972) with equal weights. Since TWI reflects the topographic nature of a watershed and CN represents the combined effect of soil types, land use, and land cover

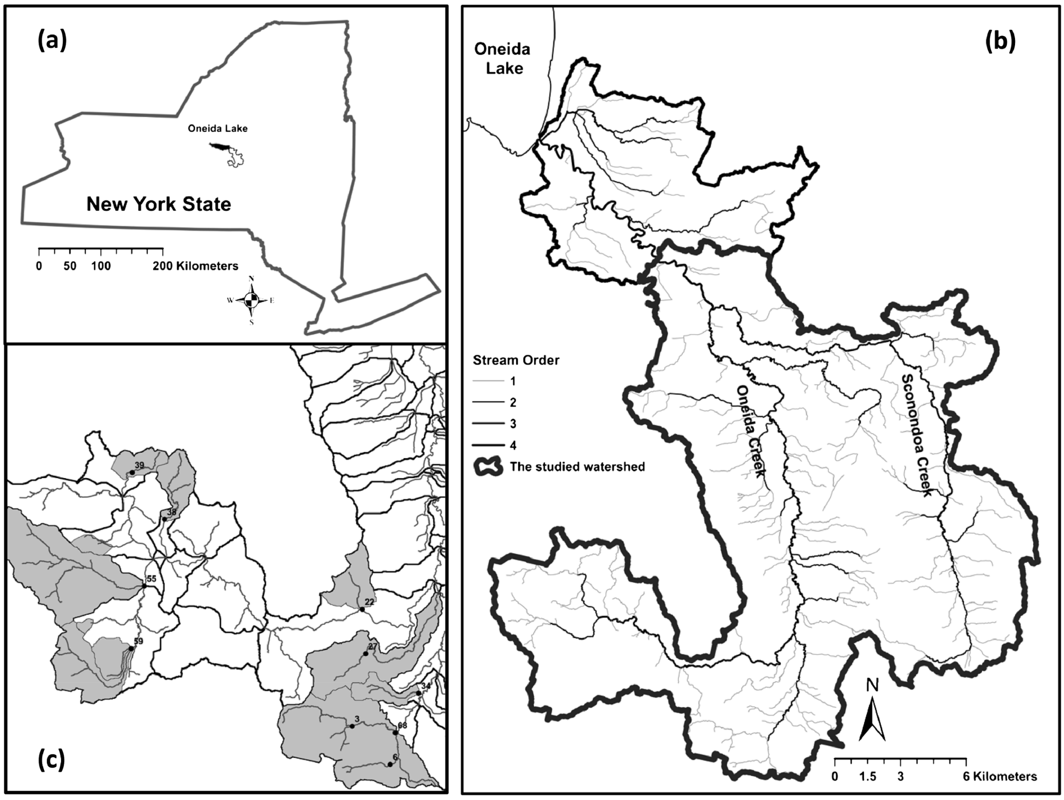

Figure 1. The location of the studied watershed and sampled SWAs. (a) The location of Oneida Creek watershed in New York State, (b) the location of the studied watershed within the Oneida Creek watershed, and (c) the sampled SWAs in the studied watershed.

on watershed hydrology, the index values are assumed to describe at the first approximation the variations of overall physiographic conditions within the watershed. A group of sub-watersheds that have the index values spanning the full range of the possible values in the studied watershed were selected. Their suitability for sampling was subsequently confirmed based on field accessibility and permission of land owners.

Automatic pumping (AP) samplers (ISCO 6712) were installed to collect water samples of one rainfall event for each selected sub-watershed and several events at the outlet, respectively. The sampler was triggered by a pre-determined threshold stage measured by the attached pressure transducer. Both the threshold stage and sampling interval were carefully selected to ensure the samples cover the full range of the event hydrograph. After the sampled event, sample bottles were replaced and transferred to the Physical Geography Laboratory at Syracuse University. The standard gravimetric method was subsequently used to obtain the corresponding suspended sediment concentrations. The stage of flow at the sampling cross-section was recorded at the 15-minute interval and downloaded into a laptop. Not only did it provide a reference for determining the time at which each sediment sample was taken, but also could be used to calculate water discharge associated with each collected sediment sample.

The geomorphologic properties of each selected site were obtained by measuring channel cross-section profile, local channel bed slope, and bed material distribution. The first two were measured with the guide of traditional surveying methods and procedures (Harrelson *et al.*, 1994). Channel cross-section survey must include the point where the stage was recorded by the AP sampler during the event. This relates the cross-section profile to the recorded stage, which will be used to calculate the associated water discharge at the cross-section. Bed material size distribution was measured using the Wolman Pebble Count method (Wolman, 1954). Based on the measured data, water discharge at each site for each recorded stage was calculated using the reference reach spreadsheet v4.2 level developed for channel survey management (Mecklenburg, 2006). Discharges at the outlet were determined by relating measured discrete values to those at the USGS gauging station. The rainfall data were obtained from the National Oceanic and Atmospheric Administration (NOAA) and a local volunteer rainfall network.

Calculation of suspended sediment loads

Averaged sediment concentration, C_m (in mg/L), and water discharge, Q_m (in m^3/s), for each sampled sub-watershed during one rainfall event were calculated using:

$$C_m = \sum_{i=1}^{n} Q_{si} t_i \Big/ \sum_{i=1}^{n} Q_i t_i \tag{1a}$$

$$Q_m = \sum_{i=1}^{n} Q_i t_i \Big/ \sum_{i=1}^{n} Q_i t_i \tag{1b}$$

where t_i is the time interval between two consecutive samples, and n is the number of samples collected during the event. Paired values of C_m and Q_m were then used with proper unit conversion factors to determine event-averaged area-specific sediment load, $Q_{S/A}$ (in kg/km^2/hr), $Q_{S/A} = C_m Q_m / A$, where A is the area of the sub-watershed. These data were subsequently used to develop an empirical equation for $Q_{S/A}$ of SWAs. Data collected at the outlet were used to establish sediment rating curves for estimating event sediment yields.

GIS determination of sediment-related parameters

Previous studies have shown that hydrological processes can be sufficiently represented using only three to five environmental parameters (Beven, 1989; El Hassanin *et al.*, 1993; Jakeman and Hornberger, 1993; Limbrunner *et al.*, 2005). Following this wisdom, we selected in order to develop an empirical equation three main environmental parameters that commonly influence sediment transport (Yang *et al.*, 2003; Dijk and Bruijnzeel, 2005; Mishra *et al.*, 2007), the mean slope of a sub-watershed, S, the percent of cropland in a sub-watershed, P, and the soil erodibility factor, K. Slope (S) is a critical individual factor that controls the degree of soil erosion. It not only directly affects soil erosion rate (El Hassanin *et al.*, 1993; Knighton, 1998) but also indirectly influences erodibility by affecting spatial heterogeneity of soil moisture, vegetation patterns, and flow patterns (Stieglitz *et al.*, 1997). Values of S for all sub-watersheds were calculated using the GIS technique based on the downloaded digital elevation model (DEM) data. National Land Cover Dataset (30 m resolution) was downloaded to calculate P for each sub-watershed. Parameter P reflects the significant influence of vegetation cover on soil erosion at the watershed scale (Kirkby and Cox, 1995). Soil erodibility factor (K) characterizes soil properties such as soil texture, structure, organic matter and permeability (Yang *et al.*, 2003) and has been used in Universal Soil Loss Equation (USLE) model to represent soil erodibility (Wischmeier and Smith, 1965). From the hydraulic perspective, Soil erodibility factor stands for soil resistance to flow and thus plays the same role as the threshold value of shear stress at which soil begins to be entrained by surface runoff. The original values of K were downloaded from Natural Resources Conservation Service (NRCS) GIS Data Mart and were aggregated into each sub-watershed. Values of each parameter were averaged within each sub-watershed, such that one sub-watershed is associated with one set of all three parameters.

Data analysis

Sediment load estimation at different spatial scales

According to the definition of SWA, event-averaged area-specific sediment load ($Q_{S/A}$) obtained at the outlet of a SWA is equivalent to event-averaged soil erosion rate per unit area from that SWA. Therefore, $Q_{S/A}$ may be termed as event-averaged unit soil erosion rate. Using data collected from sampled SWAs, we explored the empirical relationship between $Q_{S/A}$ and rainfall intensity, as well as the three environmental parameters. Theoretically, sediment transport is a function of erosivity (i.e. the driving force) and erodibility (i.e. the resistance) (Bocco, 1991). This function has been empirically expressed as the multiplication of five variables representing both erosivity and erodibility in the USLE model (Wischmeier and Smith, 1978). Following the same line, we assumed that $Q_{S/A}$ can be characterized by a function of parameters in a multiplication form and developed an empirical equation for $Q_{S/A}$.

The role of this equation is to calculate $Q_{S/A}$ for ungauged SWAs and subsequently to determine event-averaged gross erosion, E_{ea} (in kg/hr), which is defined as:

$$E_{eQ} = \sum_{i=1}^{n} \left(Q_{\frac{S}{A}}\right)_i A_i,$$

A_i is the area of one SWA and n is the number of SWAs. Utilizing this equation requires dividing the studied watershed into SWAs and the associated stream network. However, no theory or protocol is available to guide such division (Hornberger and Boyer, 1995; Devito *et al.*, 2005). Practically, sub-watersheds are often delineated at the users' discretion (Tripathi *et al.*, 2003; Mishra *et al.*, 2007; Kliment *et al.*, 2008). In this study, we identified the appropriate SWAs by examining the pattern between E_{ea} and the associated spatial scale.

Data collected at the outlet of the studied watershed were used to develop SRCs. The established SRCs were subsequently used to estimate event-based sediment loads from the entire studied watershed. These loads were subsequently used to calculate event sediment yields.

Identification of event-based sediment dynamic links

For a single rainfall event, the developed empirical equation and the appropriately delineated SWAs allowed us to determine event gross erosion. However, using the developed SRCs, we were able to compute the event sediment yield. We then compared the two and calculated event sediment delivery ratio (ESDR) for different events to identify the dominant processes controlling sediment transport between small and big events.

Results and Analysis

An empirical equation for estimating $Q_{S/A}$ and E_{ea} from SWAs

We were able to sample 16 sub-watersheds that have no more than order-three streams for one event from July to November, 2007. To identify whether all these sub-watersheds are SWAs or not, we scrutinized the obtained sediment data and the properties of these sub-watersheds in two ways. First, we analyzed the trends of scatter plots and the correlations between $Q_{S/A}$ and each of the three environmental parameters. Since S is highly correlated to $Q_{S/A}$, data points that are significantly off the main trend in the associated scatter plot were considered 'outliers' meaning the associated sub-watersheds do not appropriately represent SWAs. Second, we reviewed the laboratory analysis and revisited these sub-watersheds to check their physiographic conditions. We finally identified 10 sub-watersheds as SWAs with appropriately collected event-based data (Table I). Although they were clustered in the southwest part of the watershed (Figure 1c), the values of the three parameters in these sub-watersheds have similar ranges to those in others. Therefore, these sub-watersheds reasonably reflect the physiographic variation of the studied watershed.

Examination of the relationship between $Q_{S/A}$ and rainfall intensity showed that there is no clear correlation between the two (Figure 2), which indicates that in the studied watershed where upland hillslope is relatively well covered by vegetation, rainfall intensity does not directly influence soil erosion. This is consistent with the finding in a humid Mediterranean watershed (Nadal-Romero *et al.*, 2008) and distinguishes the studied watershed from those in arid and semi-arid regions where rainfall intensity directly contributes to soil erosion through splashing erosion on the relatively bare hillslope surface (Fang *et al.*, 2008). Consequently, we only treated the

Table I. Relevant variables of the identified and sampled SWAs.

SWA	Area (km^2)	$Q_{S/A}$ (Kg/km^2/hr)	P	K	S
CR55	8·812	0·4889	0·5231	0·2734	8·812
CR34	13·03	10·691	0·5842	0·3204	13·03
CR59	10·47	7·2295	0·5236	0·2525	10·47
CR22	11·33	8·8099	0·6706	0·2823	11·33
CR39	6·879	0·2109	0·9230	0·2757	6·879
CR38	8·695	3·7907	0·2553	0·2785	8·695
CR68	11·64	13·018	0·7353	0·2723	11·64
CR20	7·598	0·0407	0·7301	0·2713	7·598
CR27	6·273	1·3047	0·7262	0·2697	7·229
CR47	7·229	0·2463	0·5321	0·2711	6·273

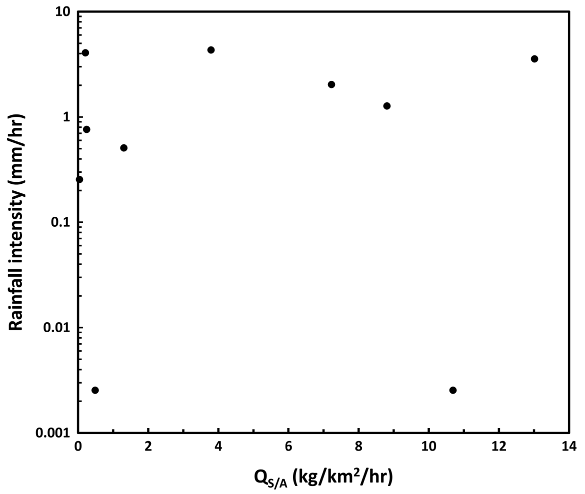

Figure 2. Plot of rainfall intensity (in mm/hr) against $Q_{S/A}$ (in kg/km^2/hr).

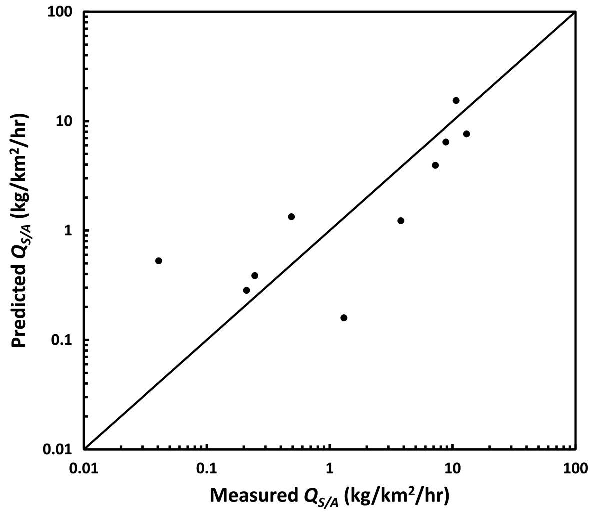

Figure 3. Predicted versus measured $Q_{S/A}$ (in kg/km^2/hr).

three environmental parameters as the independent variables. However, there may exist multiple possible sets of empirical equations that may appropriately describe the set of measured $Q_{S/A}$ values, a well-known issue termed equifinality (Beven and Freer, 2001; Beven, 2006). This problem was solved by proposing two possible candidates that have the most complex and simplest forms

$$Q_{\frac{S}{A}} = a_1 P^{a2} S^{a3} K^{a4} \tag{2a}$$

$$Q_{\frac{S}{A}} = b_1 S^{b\,2} \tag{2b}$$

where a_1, a_2, a_3, a_4, b_1, and b_2 are coefficients to be determined statistically.

Natural logarithm transformation was applied to the two equations and fitted to the data. The results indicated (Table II) that though Equation (2a) had a slightly higher R^2 value than Equation (2b), the latter produced a better adjusted R^2 than the former. Additionally, the two regression coefficients in Equation (2b) were statistically significant, whereas only that of S in Equation (2a) was (Table II). These regression outcomes indicated that both P and K were not useful explanatory variables or predictors for $Q_{S/A}$. Furthermore, the negative values of two coefficients in Equation (2a) (i.e. a_2 and a_4) implied that (i) more cropping would lead to less sediment load and (ii) higher erosion would cause less sediment produced. Both are at odds with the physical processes of erosion. Thus, $Q_{S/A}$ from SWAs may be sufficiently characterized by the mean slope, S. Although R^2 (0.60) for Equation (2b) was not high, the variation in the prediction was primarily caused by SWAs with smaller values of $Q_{S/A}$ (Figure 3), which have less contribution to event-averaged gross erosion (E_{ea}). Accordingly, Equation (2b) is an adequate empirical equation to calculate $Q_{S/A}$ in all SWAs within the studied watersheds.

Determination of the spatial scale for SWA delineation

To identify the most appropriate SWAs, we delineated the studied watershed using ArcHydro (Maidment, 2002) at six different spatial scales. With the increase of the scale, E_{ea} decreases and finally levels off (Figure 4) suggesting that E_{ea} is affected by the selection of the scale. Generally, three zones can be identified based on the trend of E_{ea} variation (Figure 4). Zone 1 involves two scales represented by the median areas of two sets of sub-watersheds, 0·611 and 0·933 km^2, respectively. At these two scales, the delineated sub-watersheds are so small (the largest sub-watersheds are 3·203 and 3·960 km^2, respectively) that many of them only contain order-one stream channels. The spatial structure of the studied watershed is not effectively reduced at these scales. Zone 3 includes two large scales at which the median areas of the delineated sub-watersheds are

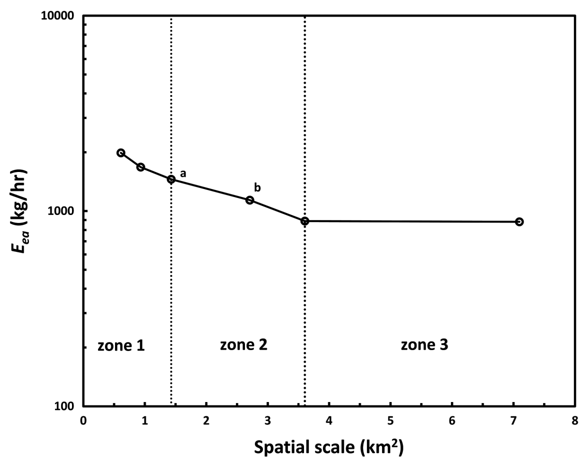

Figure 4. Impact of spatial scales on the event-averaged gross erosion, E_{ea} (in kg/hr). Each scale is represented by the median area of the delineated sub-watersheds.

Table II. Fitting statistics and coefficient estimates of the two candidate equations.

	a_1	b_1	a_2	b_2	a_3	a_4	R^2	Adjusted R^2
Equation 2a	$1{\cdot}40 \times 10^{-8}$ (0·266)		−0·85 (0·579)		6·41 (0·029)	−3·09 (0·751)	0·63	0·45
Equation 2b		$1{\cdot}63 \times 10^{-6}$ (0·0099)		6·25 (0·0083)			0·60	0·55

Note: values in parentheses are p-values.

3·606 and 7·096 km^2, respectively. At these two scales, the stream network is oversimplified and several order-three stream reaches are inappropriately eliminated. In addition, their maximum sub-watersheds are as high as 17·147 and 16·119 km^2, which are more than 5% of the total area of the studied watershed. Therefore, sub-watersheds at these scales are generally too big to be SWAs. Apparently, the most appropriate spatial scale should be within Zone 2 (Figure 4). Because E_{ea} values at the two scales are not significantly different from each other, the scales *a* or *b* do not affect the following analysis. However, comparison of area distribution at either scale with that of the sampled SWAs shows that the distribution pattern at scale *a* is much more consistent with that of the sampled SWAs than that at scale *b*. Therefore, the delineated sub-watersheds at scale *a* may be reasonably regarded as appropriate SWAs. At this scale, the studied watershed can be divided into 182 SWAs with the median size of 1·429 km^2 (Figure 5). The event-averaged gross erosion (E_{ea}) will be calculated based on these SWAs.

Sediment rating curves (SRCs) at the outlet of the studied watershed

Sediment samples, collected at the outlet of the studied watershed for four different rainfall events, involved discharges spanning from 0·91 to 25 m^3/s, which cover almost the full range of those in the study period. Although for each event, data could be described by a different SRC, the collective of all data generally followed two different linear trends (Figure 6), which may be expressed as follow:

$$\text{Small events} \quad C = c_1 \ Q \tag{3a}$$

$$\text{Big events} \quad C = c_2 \ Q \tag{3b}$$

The definition of small and big events was based on the boundary discharge that separates the two SRCs (Figure 6) and is approximately 6 m^3/s. The results from non-linear regression analysis (Table III) displayed that both equations were statistically significant with relatively high R^2 values. Although data with larger discharges showed relatively greater scatter (Figure 6), they were not from the same event suggesting no discernable hysteresis loops during single events. Thus, sediment transport was generally controlled by two different SCRs in which the one for smaller discharges has a steeper slope. This means that smaller discharges in the main stream of the studied watershed may transport more suspended sediment than larger discharges. The apparently count-intuitive phenomenon cannot be fully understood without the knowledge of the dynamic links between upland sediment sources and downstream sediment transport.

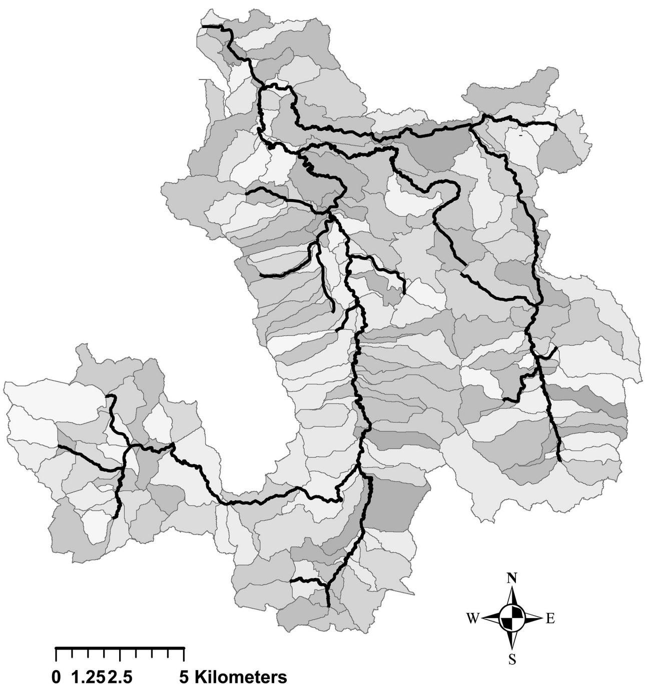

Figure 5. Delineated SWAs and the associated stream network in the studied watershed.

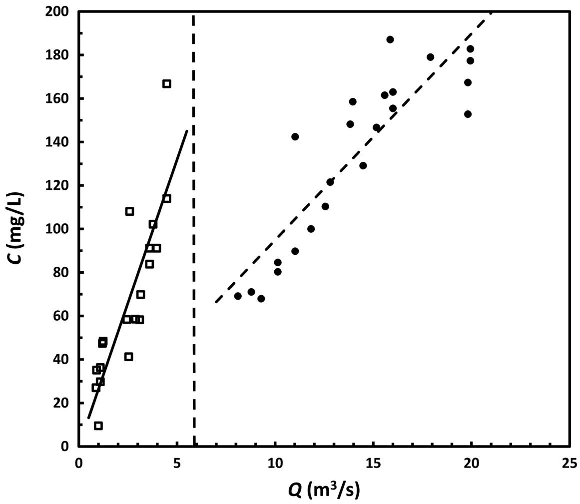

Figure 6. Two sediment rating curves (SRCs) established using the event data collected at the outlet of the studied watershed.

Event-based sediment dynamic links between sources and the downstream transport

Geomorphologically, a watershed may be viewed as the combination of hillslopes and the inter-connected stream network. With the concept of SWA, hillslopes (and their included small streams) of the studied watershed become a number of SWAs that are connected to the stream network (Figure 5). The stream network in Figure 5 is simpler than that in Figure 1 because the lower-order stream branches are 'digested' by SWAs. The event-based dynamic links between the two may be revealed using Equations (2b, 3a), and (3b).

For a given rainfall event, event gross erosion E_t (in kilograms) is the product of E_{ea} and the duration of the 'effective' surface runoff (in hours) that is large enough to transport suspended sediment (i.e. the storm flow). Unfortunately, the exact duration varies with SWAs because each SWA has a different hydrograph for the same rainfall event. Detailed durations for all SWAs require detailed field measurement in all SWAs during one event, which is practically difficult and unnecessary. An alternative is seeking a representative duration for all SWAs during a given event based on the connection between surface runoff in SWAs and the downstream discharge that can be represented

Table III. Fitting statistics and coefficient estimates of the two SRCs.

	Coefficient	R^2
Small events (Equation (3a))	26·37	0·74
Big events (Equation (3b))	9·49	0·80

by a hydrograph at the outlet. Because the storm flow of the hydrograph is primarily supplied from surface runoff on hillslopes (Bedient and Huber, 2002), the representative duration of the 'effective' surface runoff in SWAs may be reasonably denoted by the duration of storm flow in the hydrograph for the same event. In this study, the constant-slope baseflow separation method (McCuen, 2004) was used to separate the storm flow, the duration of which, T, is the representative duration of the surface runoff in all SWAs for the same event. Accordingly, E_t may be calculated by $E_t = E_{ea} T$ and the corresponding event sediment yield, SY_e (in kilograms), may be determined using either Equation (3a) or Equation (3b) for data points within the time period, T.

The study period (between July and November, 2007) was mainly comprised of 13 rainfall events in which seven were small and six were big events (Figure 7). Both E_t and SY_e were calculated using the previously described methods and compared with each other for all events. Figure 8 showed that during all small rainfall events, $E_t > SY_e$, whereas during all big events, $E_t < SY_e$. These event dynamic links between hillslope sediment supply and in-channel sediment transport provided necessary information to decipher the two different SRCs at the outlet of the watershed (Figure 6).

If $E_t = SY_e$, then all in-channel sediment supplied from SWAs during a given rainfall event is transported through the stream network. Consequently, stream channels are in equilibrium and sediment transport is (approximately) at capacity. If $E_t > SY_e$, then in-stream deposition occurs, while sediment is still transported at capacity. If $E_t < SY_e$, then the erosion process dominates and sediment is transported below capacity. During small rainfall events, water discharges in stream channels were relatively small, such that the stream power was not strong enough to carry all sediment loads supplied from all SWAs, though these sediment loads were also relatively low. As precipitation increased within small events, the difference between hillslope sediment supply (i.e. E_t) and downstream sediment load (i.e. SY_e) decreased progressively (Figure 8). This suggests that gradually more proportion of supplied sediment was transported through the stream network. The more important implication is that the rate of the increase of sediment load was faster than that of the discharge increase, which explains why the SRC for small events had a steeper slope (Figure 6).

As discharge generated by big events was greater than the threshold value (i.e. 6 m^3/s) but not very high (e.g, no more than

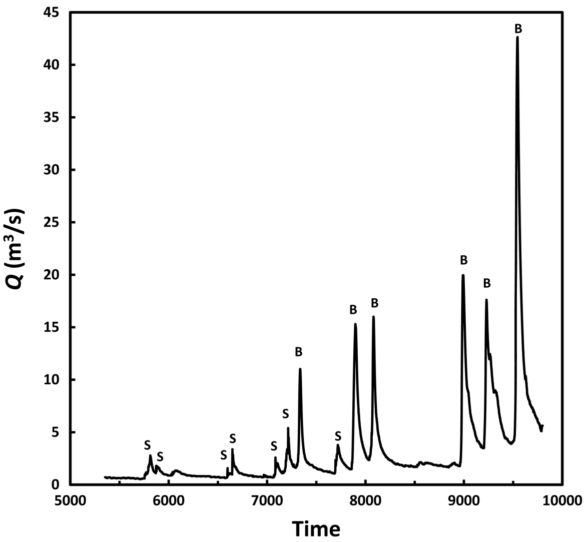

Figure 7. Identified small and big events in the studied watershed during the study period. 'S' denotes small rainfall events, whereas 'B' denotes big rainfall events.

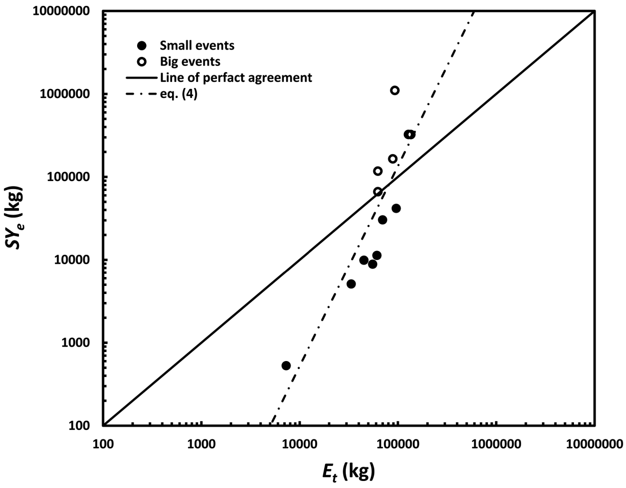

Figure 8. Comparison of event sediment yield, SY_e (in kilograms) with event gross erosion, E_t (in kilograms).

10 m^3/s) (represented by the point on the line of perfect agreement in Figure 8), stream channels were in equilibrium. The increase of precipitation within big events resulted in the increase of discharge, so fast that flow could transport more than what was supplied from SWAs. Therefore, sediment transport was below capacity. The greater discrepancy between E_t and SY_e for higher values (Figure 8) suggests that further increase of precipitation enlarged the sediment transport deficit (i.e. the increase of discharge was faster than that of sediment load in channels). This explains why the SRC for big events had a gentle slope (Figure 6). Furthermore, the greater transport deficit directly resulted in channel bank erosion that had been observed in several locations within the stream network. Thus, the two SRCs in Figure 6 reflected two different dominant processes of sediment transport during small and big events, respectively. Since SRC is commonly used to estimate sediment yield of a watershed, the different physical processes behind the two SRCs suggest that accurately estimating sediment yield of the studied watershed requires identifying small and big events first, based on which two SRCs can be used to calculate sediment loads from these events, respectively. In other words, even though discharges during the recessions of big events may be less than 6 m^3/s, which are apparently within the domain of Equation (3a), the associated sediment concentrations should be calculated using Equation (3b), because these discharges are still part of big events. For the six big events shown in Figure 8, the total sediment load should be 2191 kg when only Equation (3b) is used, whereas it becomes 2368 kg when both Equations (3a) and (3b) are used, which over-predict the load.

The general trend of the data in Figure 8 can be described by the following equation

$$SY_e = a\,E_t^{\,b} \tag{4}$$

where $a = 0{\cdot}00000012$ and $b = 2{\cdot}41$ with $R^2 = 0{\cdot}75$ ($p = 0{\cdot}0055$). The threshold value of SY_e for channels in equilibrium may be determined by setting $E_t = SY_e$, which leads to $E_t = 203{\cdot}8$ kg. Therefore, in the studied watershed, channel bank and bed erosion occurs only when the event gross erosion is greater than 204 kg and the amount of in-channel erosion can be estimated as $SY_e - E_t$. By definition, Equation (4) may also lead to an equation for ESDR: ESDR $= 0{\cdot}00000012\ E_t^{1{\cdot}41}$ indicating that sediment delivery ratio increases as the rainfall event becomes larger and larger. The general picture of event-based sediment dynamics within the studied watershed may be described as follows. During small rainfall events, sediment delivery ratio is low but in-channel sediment transport is at capacity and no channel bank and bed erosion. During big events, however, sediment delivery ratio is high while sediment transport in channels is below capacity, which encourages localized bank and bed erosion. Clearly, reducing sediment supply and protecting weak banks should be the main targets of future sediment-related watershed management practices.

Discussions

A fundamental problem tangled in understanding hydrological and sediment transport processes in a watershed is the scale issue (Zhu and Mackay, 2001; Cammeraat, 2002; Devito *et al.*, 2005; Van Dijk and Bruijnzeel, 2005; Birkinshaw and Bathurst, 2006; Brasington and Richards, 2007; García-Ruiz *et al.*, 2010). Based on data complied over the world, de Vente *et al.* (2007) demonstrated that specific sediment yield (SSY) is essentially scale dependent. In particular, SSY generally shows a complex non-linear relationship with watershed area (A) that always includes a positive trend for relatively small areas and a negative trend for relatively big areas. The specific processes dominating each trend depend on characteristics of climate, lithology, topography, and land covers in a watershed. Although the complex non-linear SSY–A curve may be significantly different in different regions of the world (see figure 5 in de Vente *et al.*, 2007), it should have similar patterns in watersheds of similar environmental conditions. This is evidenced by comparing the SSY value of the entire studied watershed (the solid triangle) to those of larger sub-watersheds (the open rectangles) in Susquehanna River Basin, Pennsylvania (Figure 9), because both watersheds have similar humid climatic and physiographic conditions. At smaller spatial scales, however, not only SSYs from SWAs of our watershed are significantly lower than those in the Pennsylvania watershed, but also the SSY–A curve in ours has a much steeper slope than that in the latter. The lower SSYs in our watershed may be because rill and sheet erosion at these scales dominates sediment transport in the Pennsylvania watershed (Osterkamp and Toy, 1997), while not in ours because of better ground coverage. The steep curve in our watershed might reflect the fact that our SSYs were calculated based on event-based data, while those in the Pennsylvania watershed were determined based on long-term averaged sediment data. The high variation of event-based sediment loads may be effectively 'smoothed out' when they are averaged over a longer time scale (Hicks, 1994). This is further confirmed by the linear relationship between long-term SSY and slope in watersheds where slope serves as the major factor to control sediment transport (Mano *et al.*, 2009; Verbist *et al.*, 2010).

Nonetheless, SSYs based on our event data clearly show a positive relationship with A at smaller spatial scales and suggest a decreasing tendency at the largest scale. This implies that sediment transport in our watershed also follows the general trend revealed by de Vente *et al.* (2007). It is thus reasonable to expect that SSY should peak at the area greater than those of SWAs where our data were collected (Figure 9). It follows that SWA represents the spatial scale that is less than the threshold area, A_c at which SSY peaks (if a watershed has two peaks as shown in figure 6C in de Vente *et al.*, 2007, then two different sets of SWAs should be used to characterize the dominant processes around each peak). Because each watershed has its own non-linear SSY–A curve (de Vente *et al.*, 2007), the specific value of A_c varies from watershed to watershed. Therefore, identification of SWAs in other watersheds should not be limited by the specific areas of SWAs in our watershed. Theoretically, the concept of SWA is an explicit version of the Dominant Processes Concept (DPC) (Bloschl, 2001). The underlying significance of

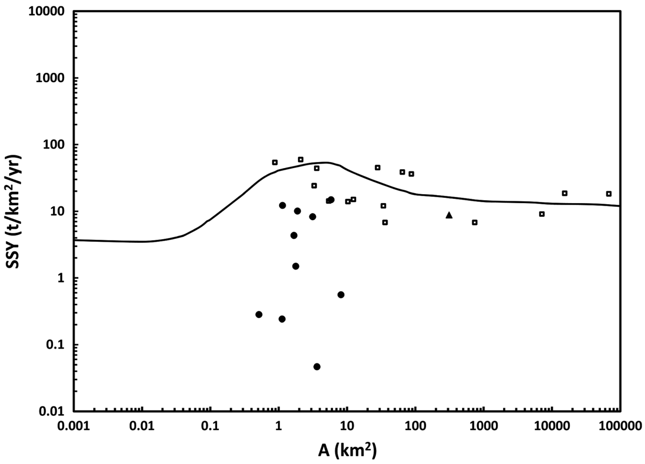

Figure 9. The relationship between specific sediment yield (SSY) and sub-watershed area (A) for the watersheds studied in this article and the Pennsylvania watersheds. The solid curve was reproduced from Osterkamp and Toy (1995). The open rectangles (□) were also reproduced from the same source. The results were used to compare with the studied SSY for the entire watershed, which is represented by the solid triangle (▲). The solid dots (•) are SSYs of our sampled SWAs. SSY values for sampled SWAs and the studied watershed were calculated by multiplying event sediment yield, SY_e, by the total hours of storm flows in one year, T_t, and then dividing the product by the area of the SWA and the total watershed area, respectively. The value for T_t was estimated by summing the hours of storm flows shown in Figure 7 and assuming that T_t is proportional to the sum.

SWA is that regardless of the specific erosion processes within a SWA (e.g. rill and sheet erosion on hillslope or channel incision or the combination of the two), the comprehensive impact of these processes may be simply evaluated by collecting data at the outlet of these SWAs.

The event-based sediment dynamic links revealed in our watershed belong to the type I and class C connectivity (Jain and Tandon, 2010), which means that our watershed is an actively connected system with a large space – short-time scale. The compartments of the system (i.e. SWAs and the main stream channels) are physically connected with one-way material transfer (i.e. water and sediment downward movement). Sediment connectivity in such a system has been commonly studied either using event-based watershed models (Borah and Bera, 2004) or by collecting detailed sediment data (Francke *et al.*, 2008). Our approach differs from these by defining and identifying SWAs, which allow for separating erosion-dominated sediment sources from deposition-controlled downstream sediment transport in our case. The separation potentially facilitates a variety of sediment-related studies in these systems, such as determining the event-based channel bank and bed erosion as achieved in this study and estimating event sediment storage of a watershed.

The developed empirical equation (i.e. Equation (2b)) involves certain uncertainty because of the small sample size. However, this uncertainty only affects the accuracy of event-averaged unit soil erosion rates ($Q_{S/A}$) calculated using Equation (2b), not the findings of the dynamic links between sediment sources and downstream sediment transport. For example, developing Equation (2b) using non-linear regression (rather than log-linear regression) would result in a different set of b_1 and b_2 for Equation (2b). Even though the event gross erosion (E_t) may be slightly different, the dynamic links revealed by comparing E_t with event sediment yield (SY_e) remain the same. More importantly, akin to the fact that each watershed has a unique non-linear SSY–A curve, each watershed must have its unique empirical equation for characterizing $Q_{S/A}$ of its SWAs. Therefore, transferring the proposed approach to a different watershed does not mean use of Equation (2b) directly, rather, it means to establish a unique empirical equation for that watershed. For example, in the earlier-mentioned Pennsylvania watershed, the empirical equation may include percentage of disturbed lands, as well as slope, while in a semi-arid watershed, it may involve rainfall intensity besides slope. Therefore, the proposed approach of linking event sediment sources to downstream sediment transport is not fundamentally affected by the uncertainty in the developed empirical equation (i.e. Equation (2b)). This, however, by no means suggests the completion of this approach. At least two further studies should be performed in the future: (i) collecting more sediment data from additional SWAs and in different seasons to test the robustness of Equation (2b); (ii) obtaining sediment data from relatively larger spatial scales to identify the peak SSY, which may help to determine the range the SWAs may have in the studied watershed.

Conclusions

Using the event data collected between July and November, 2007 at different spatial scales and the outlet of the studied watershed in central New York, we proposed a new approach to identify event-based dynamic links between sediment sources and downstream sediment transport. The approach is based on a new concept of spatial scale, SWA. SWA is defined as the sub-watershed within which all eroded soils are carried through it without deposition during a hydrological event. SWAs are sub-watersheds that have variable sizes, but these sizes must be less than the threshold area at which SSY climaxes in the SSY–A relationship where A is the area of a sub-watershed. In our humid watershed with relatively good ground cover, the approach may be summarized as follow:

1. Event-averaged unit soil erosion rate, $Q_{S/A}$ (in kg/km^2/hr), for all SWAs may be calculated using the developed empirical equation (Equation (2b))

   $$Q_{\frac{S}{A}} = 0.00000163 S^{6.2569}$$

   where S is the area-weighted mean slope of a SWA.

2. The studied watershed may be appropriately divided into 182 SWAs. Using Equation (2b) and the areas of these SWAs, we can calculate event-averaged gross erosion, E_{ea} (in kg/hr), for all rainfall events in the study period. By determining average event duration, T (in hours), using the hydrograph at the watershed outlet, we can calculate event gross erosion, E_t (kg), using $E_t = E_{ea}T$.
3. Event sediment yield, SY_e (in kilograms), may be calculated using T and the following two sediment rating curves developed at the outlet (Equations (3a) and (3b)).

   $$\text{Small events } C = 26{\cdot}37Q$$

   $$\text{Big events } \quad C = 9{\cdot}49Q$$

   where C is sediment concentration, Q is the associated water discharge, and small events are distinguished from big ones if the associated peak discharges are less than 6 m^3/s.

4. Comparison of E_t with SY_e gave rise to Equation (4)

   $$SY_e = 0{\cdot}00000012 E_t^{2{\cdot}41}$$

   Equation (4) may further lead to an equation for ESDR: $ESDR = 0{\cdot}00000012 E_t^{1{\cdot}41}$. These results divulged the following event dynamic links. During small rainfall events, sediment delivery ratio is low but in-channel sediment transport is at capacity and no channel bank and bed erosion. The rate of the increase of sediment load was faster than that of the discharge increase resulting in the higher coefficient in Equation (3a). During big events, however, sediment delivery ratio is high while sediment transport in channels is below capacity, which encourages localized bank and bed erosion. The increase of discharge was faster than that of sediment in channels leading to the lower coefficient in Equation (3b). Moreover, the event in-channel erosion can be estimated as $SY_e - E_t$.

Successful application of this approach to a different watershed relies on two critical steps: (i) developing a specific empirical equation for the watershed; and (ii) determining the appropriate SWAs of the watershed.

Acknowledgments—This research was partially supported by the Summer Project Assistantship Program sponsored by Maxwell School of Citizenship and Public Affairs at Syracuse University. The authors thank the associate editor and two anonymous reviewers for providing helpful suggestions.

References

Aksoy H, Kavvas ML. 2005. A review of hillslope and watershed scale erosion and sediment transport models. *Catena* **64**: 247–271.

Bedient PB, Huber WC. 2002. *Hydrology and Floodplain Analysis*. Prentice Hall: Upper Saddle River, NJ.

Beven KJ. 1989. Changing ideas in hydrology – the case of physically based models. *Journal of Hydrology* **105**: 157–172.

Beven KJ. 1997. TOPMODEL: a critique. *Hydrological Processes* **11**: 1069–1085.

Beven KJ. 2002. Towards an alternative blueprint for a physically based digitally simulated hydrologic response modelling system. *Hydrological Processes* **16**: 189–206.

Beven KJ. 2006. A manifesto for the equifinality thesis. *Journal of Hydrology* **320**: 18–36.

Beven KJ, Freer J. 2001. Equifinality, data assimilation, and uncertainty estimation in mechanistic modelling of complex environmnetal systems using the GLUE methodology. *Journal of Hydrology* **249**: 11–29.

Beven KJ, Kirkby MJ. 1979. A physically based, variable contributing area model of basin hydrology. *Hydrological Sciences Bulletin* **24**: 43–69.

Bilotta GS, Brazier RE. 2008. Understanding the influence of suspended solids on water quality and aquatic biota. *Water Research* **42**: 2849–2861.

Birkinshaw SJ, Bathurst JC. 2006. Model study of the relationship between sediment yield and river basin area. *Earth Surface Processes and Landforms* **31**: 750–761.

Bloschl G 2001. Scaling in hydrology. *Hydrological Processes* **15**: 709–711.

Bloschl G, Grayson RB, Sivapalan M. 1995. On the representative elementary area (REA) concept and its utility for distributed rainfull–runoff modelling. *Hydrological Processes* **9**: 313–330.

Bocco G 1991. Gully erosion: processes and models. *Progress in Physical Geography* **15**: 392–406.

Bongartz K 2003. Applying different spatial distribution and modelling concepts in three nested mesoscale catchments of Germany. *Physics and Chemistry of the Earth* **28**: 1343–1349.

Borah DK, Bera M. 2004. Watershed-scale huydrologic and nonpoint-source pollution models: review of applications. *Transactions of the American Society of Agricultural Engineers* **47**: 789–803.

Brasington J, Richards K. 2007. Reduced-complexity, physically-based geomorphological modelling for catchment and river management. *Geomorphology* **90**: 171–177.

Cammeraat LH. 2002. A review of two strongly contrasting geomorphological systems within the context of scale. *Earch Surface Processes and Landforms* **27**: 1201–1222.

Carpenter TM, Georgakakos KP. 2006. Intercomparison of lumped versus distributed hydrologic model ensemble simulations on operational forecast scales. *Journal of Hydrology* **329**: 174–185.

Central New York Regional Planning and Development Board (CNYRPDB). 2004. *A Management Strategy for Oneida Lake and its Watershed*. CNYRPDB: Syracuse, NY.

Collins AL, Walling DE. 2004. Documenting catchment suspended sediment sources: problems, approaches and prospects. *Progress in Physical Geography* **28**: 159–196.

De Roo APJ. 1998. Modelling runoff and sediment transport in catchments using GIS. *Hydrological Processes* **12**: 905–922.

Devito K, Creed I, Gan T, Mendoza C, Petrone R, Silins U, Smerdon B. 2005. A framework for broad-scale classification of hydrologic response units on the Boreal Plain: is topography the last thing to consider? *Hydrological Processes* **19**: 1705–1714.

Dijk AIJM, Bruijnzeel LA. 2005. *Key Controls and Scale Effects on Sediment Budgets: Recent Findings in Agricultural Upland Java, Indonesia*. IAHS Publication No. 292. IAHS Press: Wallingford; 24–31.

Dooge JC. 1968. The hydrologic cycle as a closed system. *Bulletin of International Society of Science and Hydrology* **13**: 58–68.

El Hassanin A, Labib T, Gaber E. 1993. Effect of vegetation cover and land slope on runoff and soil losses from the watersheds of Burundi. *Agriculture, Ecosystems and Environment* **43**: 301–308.

Fang H, Chen H, Cai Q, Li Q. 2008. Scale effect on sediment yield from sloping surfaces to basins in hilly loess region on the Loess Plateau in China. *Environmental Geology* **33**: 1977–1992.

Flugel W-A 1995. Delineating hydrological response units (HRUs) by GIS analysis regional hydrological modeling using PRMS/MMS in the drainage basin of the river Brol, Germany. *Hydrological Processes* **9**: 423–436.

Francke T, López-Tarazón JA, Vericat D, Bronstert A, Batalla RJ. 2008. Flood-based analysis of high-magnitude sediment transport using a non-parametric method. *Earch Surface Processes and Landforms* **33**: 2064–2077.

Fryire KA, Brierley GJ, Preston NJ, Kasai M. 2007. Buffers, barriers and blankets: the (dis)connectivity of catchment-scale sediment cascades. *Catena* **70**: 49–67.

Gao P 2008. Understanding watershed suspended sediment transport. *Progress in Physical Geography* **32**: 243–263.

García-Ruiz JM, Lana-Renault N, Beguería S, Lasanta T, Regüés D, Nadal-Romero E, Serrano-Muela P, López-Moreno JI, Alvera B, Martí-Bono C, Alatorre LC. 2010. From plot to regional scales: interactions of slope and catchment hydrological and geomorphic processes in the Spanish Pyrenees. *Geomorphology* **120**: 248–257.

Gauthiera V, Gérardb B, Portalb J, Blocka J, Gatelc D. 1999. Organic matter as loose deposits in a drinking water distribution system. *Water Research* **33**: 1014–1026.

Harrelson CC, Rawlins CL, Potyondy JP. 1994. *Stream Channel Reference Sites: An Illustrated Guide to Field Technique*, General Technical Report RM-245. United States Department of Agriculture, Forest Service: Fort Collins, CO.

Hicks DM. 1994. *Land-use Effects on Magnitude-frequency Characteristics of Storm Sediment Yields: Some New Zealand Examples*. IAHS Publication No. 224. IAHS Press: Wallingford; 395–402.

Hornberger GM, Boyer EW. 1995. Recent advance in watershed modelling. *Reviews of Geophysics* **33**: 949–957.

Jain V, Tandon SK. 2010. Conceptual assessment of (dis)connectivity and its application to the Ganga River dispersal system. *Geomorphology* **118**: 349–358.

Jakeman AJ, Hornberger GM. 1993. How much complxity is warranted in a rainfall–runoff model? *Water Resources Research* **29**: 2637–2649.

Jetten V, Govers D, Hessel R. 2003. Erosion models: quality of spatial predictions. *Hydrological Processes* **17**: 887–900.

Keesstra SD, van Dam O, Verstraeten G, van Huissteden J. 2009. Changing sediment dynamics due to natural reforestation in the Dragonja catchment, SW Slovenia. *Catena* **78**: 60–71.

Kirkby MJ, Cox NJ. 1995. A climatic index for soil erosion potential (CSEP) including seasonal and vegetation factors. *Catena* **25**: 333–352.

Kliment Z, Kadlec J, Langhammer J. 2008. Evaluation of suspended load changes using AnnAGNPS and SWAT semi-empirical erosion models. *Catena* **73**: 286–299.

Knighton D. 1998. *Fluvial Forms & Processes, A New Perspective*. Arnold: London.

Langlois JL, Johnson DW, Mehuys1 GR 2005. Suspended sediment dynamics associated with snowmelt runoff in a small mountain stream of Lake Tahoe (Nevada). *Hydrological Processes* **19**: 3569–3580.

Lecce SA, Pease PP, Gares PA, Wang J. 2006. Seasonal controls on sediment delivery in a small coastal plain watershed, North Carolina, USA. *Geomorphology* **73**: 246–260.

Lefran J, Grimaldi C, Gascuel-Odoux C, Gilliet N 2007. Suspended sediment and discharge relationships to identify bank degradation as a main sediment source on small agricultural catchments. *Hydrological Processes* **21**: 2923–2933.

Limbrunner JF, Vogel RM, Chapra SC. 2005. A parsimonious watershed model. In *Watershed models*, Singh VP, Frevert DK (eds). Taylor & Francis Group: Boca Raton, FL.

Maidment DR. 2002. *Arc Hydro, GIS for Water Resources*. ESRI: Redland.

Makarewicz JC, Lewis TW. 2003. *Nutrients and Suspended Solid Losses from Oneida Lake Tributaries, 2002–2003*. Central New York Regional Planning and Development Board: Syracuse, NY.

Mano V, Nemery J, Belleudy P, Poirel A. 2009. Assessment of suspended sediment transport in four alpine watersheds (France): influence of the climatic regime. *Hydrological Processes* **23**: 777–792.

Martinez-Carreras N, Krein A, Udelhoven T, Gallart F, Iffly JF, Hoffmann L, Pfister L, Walling DE. 2010. A rapid spectral-reflectance-based fingerprinting approach for documenting suspended sediment sources during storm runoff events. *Journal of Soils and Sediments* **10**: 400–413.

McCuen R 2004. *Hydrologic Analysis and Design*. Pearson Prentice Hall: Upper Saddle River, NJ.

Mecklenburg D 2006. Division of Soil and Water Conservation: STREAM Modules. Retrieved 10 1. Ohio Department of Natural Resources: Columbus, OH. http://ohiodnr.com/?TabId=9188

Medeiros PHA, Guntner A, Francke T, Mamede GL, de Araujo JC. 2010. Modeling spatio-temporal patterns of sediment yield and connectivity in a semi-arid catchment with the WASA-SED model. *Hydrological Sciences Journal* **55**: 636–648.

Merritt WS, Letcher RA, Jakeman AJ. 2003. A review of erosion and sediment transport models. *Environmental Modelling and Software* **18**: 761–799.

Merz B, Plate EJ. 1997. An analysis of the effects of spatial variability of soil and soil moisture on runoff. *Water Resources Research* **33**: 2909–2922.

Mishra A, Kar S, Singh VP. 2007. Prioritizing structural management by quantifying the effect of land use and land cover on watershed runoff and sediment yield. *Water Resources Management* **21**: 1899–1913.

Mizugaki S, Onda Y, Fukuyama T, Koga S, Asai H, Hiramatsu S. 2008. Estimation of suspended sediment sources using Cs-137 and Pb-210 (ex) in unmanaged Japanese cypress plantation watersheds in southern Japan. *Hydrological Processes* **22**: 4519–4531.

Moreno-de las Heras M, Nicolau JM, Merino-Martín L, Wilcox BP. 2010. Plot-scale effects on runoff and erosion along a slope degradation gradient. *Water Resources Research* **46**: W04503.

Nadal-Romero E, Latron J, Marti-Bono C, Regues D. 2008. Temporal distribution of suspended sediment transport in a humid Mediterranean badland area: the Araguás catchment, central Pyrenees. *Geomorphology* **97**: 601–616.

Oeurng C, Sauvage S, Sánchez-Pérez J. 2010. Dynamics of suspended sediment transport and yield in a large agricultural catchment, southwest France. *Earch Surface Processes and Landforms* **35**: 1289–1301.

Oreskes N, Shrader-Frechette K, Belite K. 1994. Verification, validation, and confirmation of numerical models in the earth sciences. *Science* **263**: 641–646.

Osterkamp WR, Toy TJ. 1997. Geomorphic considerations for erosion prediction. *Environmental Geology* **29**: 152–157.

Owens PN, Batalla RJ, Collins AJ, Gomez B, Hicks DM, Horowitz AJ, Kondolf GM, Marden M, Page MJ, Peacock DH, Petticrew EL, Salomons W, Trustrum NA. 2005. Fine-grained sediment in river systems: environmental significance and management issues. *River Research and Applications* **21**: 693–717.

Pimentel D, Harvey C, Resosudarmo P, Sinclair K, Kurz D, McNair M, Crist S, Shpritz L, Fitton L, Saffouri R, Blair R. 1995. Environmental and economic costs of soil erosion and conservation benefits. *Science* **267**: 1117–1123.

Quilbe R, Rousseau AN, Moquet J-S, Savary S, Ricard S, Garbouj MS. 2008. Hydrological responses of a watershed to historical land use evolution and future land use scenarios under climate change conditions. *Hydrology and Earth System Sciences* **12**: 101–110.

Ramankutty N, Foley JA. 1999. Estimating historical changes in land cover: North American croplands from 1850 to 1992. *Global Ecology and Biogeography* **8**: 381–396.

Russell MA, Walling DE, Hodgkinson RA. 2001. Suspended sediment sources in two small lowland agricultural catchments in the UK. *Journal of Hydrology* **252**: 1–24.

Rustomji P 2006. Analysis of gully dimensions and sediment texture from southeast Australia for catchment sediment budgeting. *Catena* **67**: 119–127.

Sadeghi SHR, Mizuyama T, Miyata S, Gomi T, Kosugi K, Fukushima T, Mizugaki S, Onda Y. 2008. Determinant factors of sediment graphs and rating loops in a reforested watershed. *Journal of Hydrology* **356**: 271–282.

Salant NL, Hassan MA, Alonso CV. 2008. Suspended sediment dynamics at high and low storm flows in two small watersheds. *Hydrological Processes* **22**: 1573–1587.

Salant NL, Renshaw CE, Magilligan FJ, Kaste J, Nislow K, Heimsath A. 2007. The use of short-lived radionuclides to quantify transitional bed material transport in a regulated river. *Earch Surface Processes and Landforms* **32**: 509–524.

Singh VP. 1995. Watershed modeling. In *Computer Models of Watershed Hydrology*, Singh VP (ed). Water Resources Publications: Littleton; 1–22.

Smith HG, Dragovich D. 2009. Interpreting sediment delivery processes using suspended sediment–discharge hysteresis patterns from nested upland catchments, south-eastern Australia. *Hydrological Processes* **23**: 2415–2426.

Stieglitz M, Rind D, Famiglietti J, Rosenzweig C. 1997. An efficient approach to modeling the topographic control of surface hydrology for regional and global climate modeling. *Journal of Climate* **10**: 118–137.

Strahler A 1952. Hypsometric (area altitude) analysis of erosional topology. *Geological Society of America Bulletin* **63**: 1117–1142.

Tripathi MP, Panda RK, Raghuwabshi NS. 2003. Indentification and prioritisation of critical sub-watersheds for soil conservation management using the SWAT model. *Biosystems Engineering* **85**: 365–379.

US Department of Agriculture-Soil Conservation Service (USDA-SCS). 1972. *National Engineering Handbook, Part 630 Hydrology, Section 4, Chapter 10*. Natural Resources Conservation Service, US Department of Agriculture: Washington, DC.

Van Dijk AIJM, Bruijnzeel LAS. 2005. Key controls and scale effects on sediment budgets: recent findings in agricultural upland Java, Indonesia. *Proceedings, The International Symposium on Sediment Budgets*, Foz do Iguaco, Brazil; **292**, 24–31.

de Vente J, Poesen J, Arabkhedri M, Verstraeten G. 2007. The sediment delivery problem revisited. *Progress in Physical Geography* **31**: 155–178.

de Vente J, Poesen J, Bazzoffi P, Van Rompaey A, Verstraeten G. 2006. Predicting catchment sediment yield in Mediterranean environments: the importance of sediment sources and connectivity in Italian drainage basins. *Earch Surface Processes and Landforms* **31**: 1017–1034.

Verbist B, Poesen J, van Noordwijk M, Widianto, SD, Agus F, Deckers J. 2010. Factors affecting soil loss at plot scale and sediment yield at catchment scale in a tropical volcanic agroforestry landscape. *Catena* **80**: 34–46.

Walling DE. 1999. Linking land use, erosion and sediment yields in river basins. *Hydrobiologia* **410**: 223–240.

Wilkinson SN, Prosser IP, Rustomji P, Read AM. 2009. Modelling and testing spatially distributed sediment budgets to relate erosion processes to sediment yields. *Environmental Modelling and Software* **24**: 489–501.

Williams GP. 1989. Sediment concentration versus water discharge during single hydrologic events in rivers. *Journal of Hydrology* **111**: 89–106.

Wilson CG, Kuhnle RA, Bosch DD, Steiner JL, Starks PJ, Tomer MD, Wilson GV. 2008. Quantifying relative contributions from sediment sources in conservation effects assessment project watersheds. *Journal of Soil and Water Conservation* **63**: 523–532.

Wischmeier W, Smith D. 1965. *Predicting Rainfall-Erosion Losses from Cropland East of the Rocky Mountains: Guide for Selection of Practices for Soil and Water Conservation*. Handbook No. 282. US Department of Agriculture: Washington, DC; 47.

Wischmeier WH, Smith DD. 1978. *Predicting Rainfall Erosion Losses – A Guide to Conservation Planning*. Agriculture Handbook No. 537. US Department of Agriculture: Washington DC.

Wolman M 1954. A method of sampling coarse river-bed material. *Transactions of the American Geophysical Union* **35**: 951–956.

Wood EF, Sivapalan M, Beven KJ, Bend LE. 1988. Effect of spatial variability and scale with implications to hydrologic modeling. *Journal of Hydrology* **102**: 29–47.

Woods R, Sivapalan M. 1995. Investigating the representative elementary area concept: an approach based on field data. *Hydrological Processes* **9**: 291–312.

Wren DG, Wells RR, Wilson CG, Cooper CM, Smith SJ. 2007. Sedimentation in three small erosion control reservoirs in northern Mississippi. *Journal of Soil and Water Conservation* **62**: 137–144.

Yang D, Kanae S, Oki T, Koike T, Musiake K. 2003. Global potential soil erosion with reference to land use and climate changes. *Hydrological Processes* **17**: 2913–2928.

Zhu AX, Mackay DS. 2001. Effects of spatial detail of soil information on watershed modeling. *Journal of Hydrology* **248**: 54–77.